Evaluating the resilience benefits of marine energy in microgrids

Sarah F. Newman, Dhruv Bhatnagar, Rebecca S. O'Neil, Andy P. Reiman, Danielle C. Preziuso, and Bryson Robertson

Abstract—**Marine energy resources could promote clean energy and resilience of coastal and island microgrids, and thus, these applications are a key future market for marine energy development. To demonstrate these benefits, this paper illustrates how inclusion of wave resources into energy resilience solutions can improve overall grid efficiency and sustainability, as well as maintain electricity supply during grid outages. The paper describes a case study evaluation of the potential to add wave energy to the Moloka'i grid as Hawaii strives to meet a 100% clean energy target. The Microgrid Component Optimization for Resilience tool is used to simulate operation in off-grid conditions and size different combinations of wave, solar photovoltaic (PV), wind, storage, and fuel resources required to meet resilience objectives. This research investigates how including wave resources in a microgrid contributes to reducing or eliminating biofuel generation, producing a zero-greenhouse gas emission profile in the latter case, and avoiding the over-sizing of PV and battery systems to accommodate periods of unavailability or high demand. Insight from this paper supports the value proposition of wave resources for future markets and informs the relationship between marine generators and microgrids or isolated grids.**

Index Terms—**Microgrids, Resilience, Value Proposition of Marine Energy Resources**

I. Introduction

Manuscript received December 28th, 2021, published 15 September 2022.

This work was supported by the Water Power Technologies Office at the U.S. Department of Energy under Contract DE-AC05-76RL01830.

S. F. Newman is at Pacific Northwest National Laboratory 1100 Dexter Ave. N, Suite 500, Seattle, Washington 98109, U.S.A. (e-mail: sarah.newman@pnnl.gov).

D. Bhatnagar is at Pacific Northwest National Laboratory 620 SW Fifth Ave., Suite 810, Portland, Oregon 97204, U.S.A. (e-mail: dhruv.bhatnagar@pnnl.gov

R. S. O'Neil is at Pacific Northwest National Laboratory 620 SW Fifth Ave., Suite 810, Portland, Oregon 97204, U.S.A. (e-mail: rebecca.oneil@pnnl.gov

A. P. Reiman is at Pacific Northwest National Laboratory 902 Battelle Boulevard, Richland, Washington 99354, U.S.A. (e-mail: andrew.reiman@pnnl.gov

D. C. Preziuso is at Pacific Northwest National Laboratory 902 Battelle Boulevard, Richland, Washington 99354, U.S.A. (e-mail: danielle.preziuso@pnnl.gov

B. Robertson is at Oregon State University 370 Strand Agriculture Hall Corvallis, Oregon 97331, U.S.A. (e-mail: bryson.robertson@oregonstate.edu

Digital Object Identifier: https://doi.org/10.36688/imej.5.143-150

WHERE there is a need for guaranteed continuous electric supply in the event of a grid disruption – such as energizing a community emergency center, an industrial site, or an island – there is an increasing interest in the development of renewably powered microgrids and local generating resources. Historically, these sites have relied on diesel generators, yet these resources emit greenhouse gases, require ample fuel stores, and are subject to extensive supply chain and price volatility. Additionally, the uncertainty of fuel delivery and continued resupply needs create cascading dependencies in a time of disruption and unusually high demand. Integrated PV, wind, and battery storage systems can partially replace reliance on diesel generators and help maintain a continuous power supply for extended periods. However, they introduce greater upfront costs, must be over-sized compared to actual electricity demands to ensure availability when needed, and cannot guarantee uninterrupted power supply because of uncertainties, the intermittent nature of local PV and wind resources, and limitations in the amount of energy that can be stored in on-site battery storage systems.

Because their resource availability is not tied to local conditions, marine energy resources are highly predictable and persistent when compared to other renewables such as wind and PV [1]–[3]. Rather, the availability of wave energy resources, for example, is tied to the timing and location of storm activities across the entire ocean basin under investigation, with the Pacific Ocean being the focus of the current study. These characteristics lend them favorably for potential grid applications, particularly for coastal and island power systems where their generation potential is high. Island power systems are typically supported by on-site renewable generation, on-site non-renewable generation with transported fuel, or energy transmitted via sub-sea cables connected to the mainland grid. Therefore, the robustness of grid operations depends heavily on the diversity of on-site generation resources and the reliability of the power transmission medium. Problems relating to these factors may lead to impediments in continuous and reliable operation of the power system.

Accordingly, marine energy resource technologies, including wave energy devices, tidal turbines, ocean and river current turbines, ocean thermal energy conversion, etc., have been evaluated for deployment in remote or island locations that are often reliant on fossil fuel imports. These locations include remote communities in the U.S. State of Alaska, Vancouver Island in British Columbia, and the Faroe Islands, among others [4]–[6]. Work on Vancouver island has evaluated the performance of wave energy converters, estimating their capacity factors using wave resource data and using this metric to consider their suitability to deliver energy to the island [5]. Several other studies have been conducted across different regions to characterize marine energy resource output and potential for grid integration. For example, both academic and utility evaluations in the Faroe Islands have examined the potential for tidal energy resources to help the region meet clean energy targets by complementing island PV and wind generation at seasonal scales [6]–[8]. Researchers in Italy have evaluated the potential to power small Mediterranean islands using wave and PV resources together, by characterizing wave device technology performance and matching generation to load, and predicted the resultant fuel savings and emissions reductions relative to baseline operations [9]. Other recent work, building upon prior work in Europe, has considered the potential for tidal phase diversity to produce smoother power profiles in both remote environments in Alaska and grid-connected regions in the state of Washington, to ease grid integration. This work found that although the potential exists to exploit tidal resources for this benefit, in the specific regions under study, the value may be limited [10]. Despite their potential to provide value as identified in these studies, marine energy technologies largely remain in a research and development stage, with only limited early commercialization activity. However, their value as a renewable resource that can deliver predictable and persistent energy may represent near-term opportunities for their deployment in island and remote communities as often these regions suffer from high electricity prices [5].

Prior research efforts that have evaluated the grid integration potential of marine energy devices to displace fossil resources have focused primarily on characterization of the marine energy resource. This work takes a more grid-centric approach, demonstrating the value of marine energy resources in combination with other renewables through a sensitivity analysis and showing the resilience benefits of including marine energy resources in place of building out additional PV and wind capacity. In this paper, we describe a novel methodology that quantifies the benefits of including marine energy resources in island power systems and requires minimal data inputs. Specifically, our proposed methodology only relies on typical hourly load and generation profiles as inputs and provides systematic measures to quantify associated operational risks. Subsequently, we use the formulation to evaluate the effectiveness of marine energy resources in providing resilience benefits to island power systems and how the use of marine energy compares with and complements that of other renewable resources, such as PV and wind.

We used the Hawaiian island of Moloka'i as a case study site to evaluate the resilience benefits of wave energy in an all-renewable grid. Working towards the State of Hawaii's goal of 100% renewable energy by 2045, Moloka'i was once projected to reach its own goal of 100% renewable energy by the end of 2020. Hawaiian Electric Companies' Power Supply Improvement Plans indicated that the island could reach this goal through distributed PV, utility-scale wind, and biofuel [11]. Given the near-term forecast of the analysis, marine energy technologies were not included; however, the methodology formulated here allows for the assessment of how wave energy resources could replace biofuel for a zero-emission grid. Moloka'i's north coastline has a significant incident wave potential, and at the community of Kalaupapa, an incident wave resource of 12 kW/m for more than 60% of of the time during the year [12].

II. Methodology

A. Data

To model Moloka'i's electric demand, a single one-year hourly load profile was used based on data provided from Hawaiian Electric [13]. Hourly wind production was modeled using NASA's Modern-Era Retrospective Analysis for Research and Applications, version 2 (MERRA-2), using data from the year 2014 at 40-m height. MERRA-2 is a long-term, global reanalysis product with a wide range of atmospheric data generated by combining modern forecasting systems and data assimilation [14]. While Hawaii's Power Supply Improvement Plan specified utility-scale wind in their assessment [11], which generally indicates turbines with rated capacities greater than 1 MW, a more recent request for proposal from Maui Electric Company only solicited small wind turbines up through 100 kW in size for the island of Moloka'i [15]. To reflect these specifications, the NPS 100C-24 power curve [16] was used to simulate power production for each of the hourly wind speeds in the subset of MERRA-2 data.

Wave energy resource data used for this project were provided from the Department of Energy-funded Early Market Opportunity Hot Spot Identification and Resource Characterization project. The project, a collaboration among PNNL, the National Renewable Energy Laboratory, and Sandia National Laboratories, is focused on developing the highest fidelity assessment of U.S. wave and tidal renewable energy resources. For the wave resource, PNNL and Sandia are using the SWAN model that is driven by WaveWatch III boundary conditions and CFSR winds to develop a 32-year hindcast of U.S. wave resources at hourly temporal resolution [17], [18].

The outputs from the SWAN model were post-processed according to the International Electrotechnical Commission (IEC) TC 114 62600-101: Wave Energy Resource Assessment and Characterization specifications. An IEC compliant wave energy resource assessment requires a minimum of two parameters to accurately quantify the resource: the significant wave height and the energy period. These two parameters are based on distribution of wave variance density across a wide range of frequencies and directions [19].

Correspondingly, the power output of a wave energy converter (WEC), a device that converts the potential and kinetic energy of waves into electric energy, needs to be quantified against all expected combinations of significant wave height and energy period. The performance of wave energy converter designs or architectures varies significantly across both dimensions. Two different marine energy generation technologies, specifically wave technologies, were used in these analyses; a Backwards Bent Ducted Buoy (BBDB) and a Two Body Point Absorber (2BPA) [19]–[21]. These two device types are considered to account for the current lack of technology convergence in wave devices, and as will be evident in this work, their output varies. The BBDB uses a hydro-dynamically active hull to create a pressure differential within an interior, enclosed air volume. A bi-radial air turbine power take-off (PTO) is used to convert the pressure differential vs. ambient pressure into electrical power. Conversely, the 2BPA harnesses the relative velocity differences between a hydro-dynamically active surface float and a stable, sub-surface heave plate. In this case, linear velocity constant PTO damping is used to generate electricity.

The WEC performance of the technologies used in this work are based on experimentally validated ProteusDS numerical models developed by the University of Victoria, Canada [20], [21]. ProteusDS is a time-domain, finite-element hydrodynamic solver that accounts for the dynamics of floating bodies under excitation from environmental conditions (waves, wind, currents, etc.). The WEC power output time-series data are generated by multiplying the hourly time-series of the significant wave height and energy period (from the previously noted SWAN numerical wave model) by the appropriate WEC performance matrices (which include efficiencies and loss factors) [19].

All three renewable annual generation profiles are shown in Fig. 1 for a 1MW system. Solar PV generation profiles were calculated as described in the following section.

B. Microgrid simulation

The ability of different renewable resources to meet Moloka'i's electrical load is evaluated using the Microgrid Component Optimization for Resilience (MCOR) tool, developed at PNNL [22]. MCOR uses a statistical model to simulate PV resources under a wide range of potential grid outage conditions, simulates microgrid operation for each of those profiles, and returns several different combinations of resources (including PV, batteries, and diesel generators) that can meet a site's electrical loads under all simulated outage conditions. The details of the MCOR PV profile generation algorithm and microgrid operation simulation are discussed in detail in [22]. As MCOR is designed to evaluate PV resources, considering wind and wave required some modifications, which are discussed in II-C.

The main result of an MCOR analysis is a set of microgrid configurations with resource capacities that can meet a site's load under a large range of outage conditions. These configurations range from nearly 100% renewable generation to configurations much more reliant on diesel generation. For the analysis presented here, the MCOR simulation was slightly modified to enable the comparison of how different types of renewable resources can be incorporated into a 100% renewable microgrid.

C. Simulation suite

To evaluate and compare the advantages of including different renewable energy resources in a microgrid supplying the electrical load of the island of Moloka'i, a simulation pipeline was established to run MCOR simulations iteratively and extract key metrics. In this pipeline, MCOR performed 100 simulations of an outage of 14 days to produce 100 unique PV outage profiles. The outage periods start at different times during the year and include a large variation in PV resource availability as modeled by MCOR. A base microgrid system was modeled with 3.5 MW of PV capacity, 5 MW of wind capacity, a 17-MW/136-MWh battery, and a biofuel generator supplying the remainder of the load. The PV and wind capacities were determined based on the installed capacities listed in the Moloka'i near-term resource plan [11], whereas the battery capacity was increased significantly from the Moloka'i resource plan to allow for the microgrid to significantly reduce or remove the need for biofuel generation in most simulations. The peak Moloka'i load for the year modeled, 2018, was 4.6 MW, the average load was 3.3 MW, and the annual demand was 29 GWh [13]. Several sets of simulations were run to explore how incorporating additional renewable energy resources into this baseline system (PV, wind, or wave) could reduce or eliminate the reliance on biofuel, thus reducing emissions or providing a zero-emission microgrid that uses only generating resources with no outside dependencies.

1) Renewable capacity required for zero-emissions: The first simulation set determined the additional capacity required from each renewable energy resource type to increase zero-emission energy levels to 95% and 100%. For each resource type (PV, wind, or wave), capacity was added in increments of 50 kW to the baseline microgrid system until zero-emission generation reached 95% and 100% or a maximum additional capacity of 10 MW was reached. This threshold was set to prevent the simulations from running indefinitely in the case where no additional renewable capacity was sufficient to meet all load for the outage period given the baseline battery capacity. The number of simulations for which 10 MW was not sufficient to meet all load without biofuels was recorded as well as the average required additional capacity across the 100 simulated outage periods.

For each iteration, an MCOR simulation was run on the new microgrid system to determine the amount of energy the biofuel generator was required to supply to meet all load. This was then used to calculate the zero-emission generation percentage and determine if another iteration was required. Adding PV capacity for the simulation was relatively straightforward given that MCOR is designed to model PV generation in microgrids, but for the wind and wave resources, modifications to the program were required. First, the

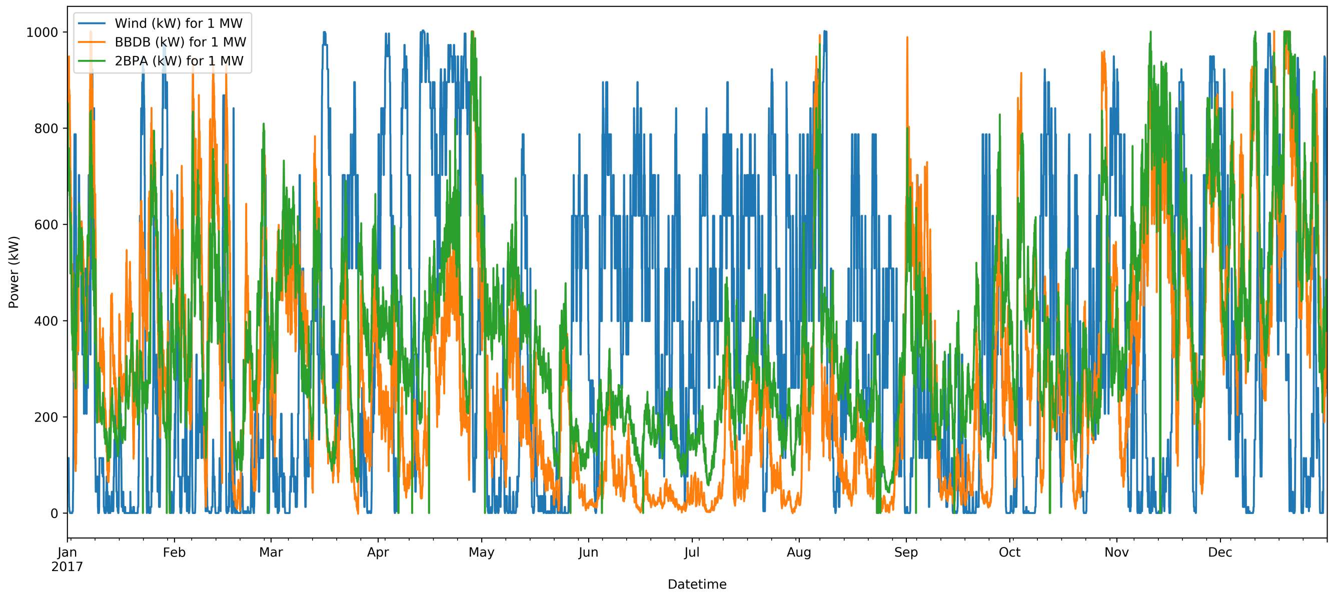

Fig. 1. Annual hourly power production in kW for a 1-MW renewable energy system with wind shown in blue, and marine energy resources shown in orange and green.

hourly wind or wave generation for a given outage period was calculated by indexing the appropriate time range from the annual generation profiles described in section II-A, then the hourly generation was scaled to the aggregated resource capacity for each resource type for the given iteration, and finally, this hourly generation was subtracted from the hourly load profile for the outage period. Then, the MCOR simulation was run as usual using this reduced hourly load.

2) Battery capacity required for zero-emissions: The second simulation set measured the additional battery capacity required to reach 100% zero-emission generation after 5 MW of renewable capacity was added to the baseline system for each of the different resource types. Battery power and capacity was added in increments of 500 kW/500 kWh until the threshold was met or a maximum battery capacity of 211 MWh was reached (corresponding to 200 iterations – at which point, adding additional battery capacity resulted in diminishing returns).

3) Biofuel requirements for fixed additional renewable capacity: The third simulation set measured the impact on biofuel usage when 5 MW of additional renewable energy capacity was added to the baseline microgrid. The metrics measured were the required generator capacity, the fuel usage, the fuel cost, and the sustainable ride-through energy ratio (SRE) [23]. For these calculations, a biofuel cost of $40.93/MMBtu was used [11]. The biofuel usage and cost were calculated using MCOR's default fuel efficiency curves. These are based on diesel fuel use, not biofuel, so those metrics may be inaccurate if the expected biofuel efficiency is significantly different, although this does not impact the generator capacity or SRE.

Note that while we are including biofuel usage and cost metrics here, we are not including a comparison of overall capital or operating costs between the different microgrid configurations. This is because robust costs for wave energy converters are currently not available, and would be required for any comparison between costs among renewable energy resources. Therefore, the focus of this review is not on the costs of various strategies, but the relative performance against several energy metrics of renewable deployment portfolios. We recognize that costs will be a decisive factor in ultimate deployment. However, the purpose of this review is to illustrate why marine energy may be worthwhile to investigate further.

SRE describes the fraction of load energy over a period of time supplied without consuming fuel [23]. Reducing fuel consumption extends the length of time that a system can operate independently and increases sustainability and resilience while reducing dependence on external supply chains. In this case, SRE is the portion of the load over a period of time served without consuming biofuel (i.e., by PV, wind, and marine energy resources).

$$SRE = 1 - \frac{E_T^{BF}}{E_T^L} \qquad (1)$$

where E_T^{BF} is the energy supplied by biofuels in time period T and E_T^L is the total load energy in time period T.

III. Results

A. Renewable capacity required for zero-emissions

For this set of simulations, additional renewable energy capacity was added to the baseline microgrid system until a fixed percentage of generation from zero-emission resources was achieved or a maximum threshold capacity was reached. Simulations were run for additional capacity from PV, wind, and wave resources (using both wave generation profiles) for 100 outage profiles each. Table I shows the percentage of simulations where the maximum additional capacity

TABLE I
PERCENT OF SIMULATIONS WHERE ADDITIONAL CAPACITY WAS INSUFFICIENT

	PV	Wind	Wave (BBDB)	Wave (2BPA)
95% renewables	52%	24%	18%	2%
100% renewables	65%	57%	38%	6%

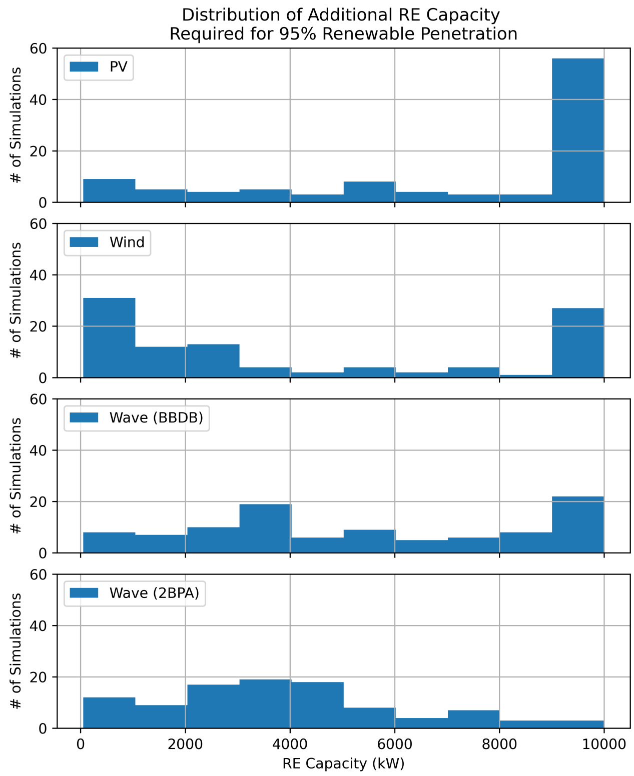

Fig. 2. The distribution of required additional renewable energy capacity required for the baseline system to achieve 95% zero-emission generation across 100 simulations. A required capacity of 10 MW indicates that the maximum number of iterations was reached before the system could meet the zero-emission generation threshold.

(10 MW) was reached before the microgrid was sufficient to meet 95% or 100% of the load without the use of biofuels. The inclusion of either wave profile resulted in the smallest number of simulations that still required some biofuel generation, although there was a large variation between the two WEC types.

This also can be seen in Fig. 2 which compares the required additional renewable capacity to achieve 95% zero-emission generation for additional PV, wind, and wave capacity. An additional capacity of 10 MW indicates that the maximum capacity was reached before 95% of the load was able to be met by zero-emission resources. Interestingly, the required wind capacity is somewhat bi-modal with either a small required additional capacity or no capacity sufficient to meet the zero-emission threshold, whereas wave generation is able to meet the zero-emission goal for a larger number of simulations, but with a higher required capacity on average.

The percent reduction in additional capacity required for wind and wave to meet 95% and 100% zero-emission generation as compared with PV is shown

TABLE II
PERCENT REDUCTION IN REQUIRED ADDITIONAL RE CAPACITY BY ADDING WIND OR WAVE INSTEAD OF PV

	Wind	Wave (BBDB)	Wave (2BPA)
95% zero-emission generation	42%	25%	47%
100% zero-emission generation	29%	15%	40%

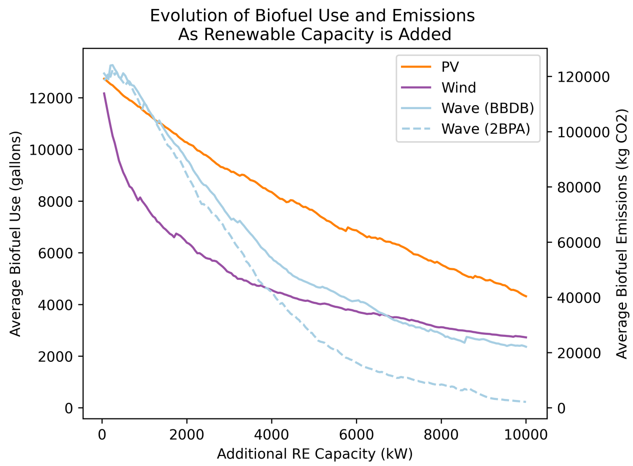

Fig. 3. The average evolution of biofuel consumption and emissions as a function of additional renewable capacity for PV, wind, and wave resources. The data is averaged over 100 independent outage profiles.

in Table II. Both wind and wave resources require a significantly lower additional capacity than PV to meet the zero-emission generation goal, with the 2BPA wave profile performing the best.

Fig. 3 shows the evolution of biofuel consumption and corresponding CO_2 emissions as more renewable energy capacity is added to the microgrid for each iteration of the simulation. The average fuel consumption and emissions across the 100 outage profiles is shown for each of renewable resource types as a function of additional capacity. To calculate CO_2 emissions from fuel consumption (which the simulation includes as an output), it was assumed that biodiesel fuel was used with an emissions factor of 73.84 kg CO_2/mmBtu [24] and an energy content of 126,700 Btu/gal [25].

Fig. 4 shows the microgrid resource dispatch operation for one of the outage profiles for the baseline system (a) and with the addition of 5 MW of PV (b), wind (c), or wave (d) capacity, using the 2BPA profile. In all four plots, the required biofuel energy production is shown in red. Even though the same renewable energy capacity is added to the baseline in plots (b), (c), and (d), the required biofuel production is much lower with the addition of wind capacity compared with PV, and wave capacity compared with both PV and wind. This is because adding a more diverse mix of renewable resources increases the likelihood that at least one resource is producing energy at any given time.

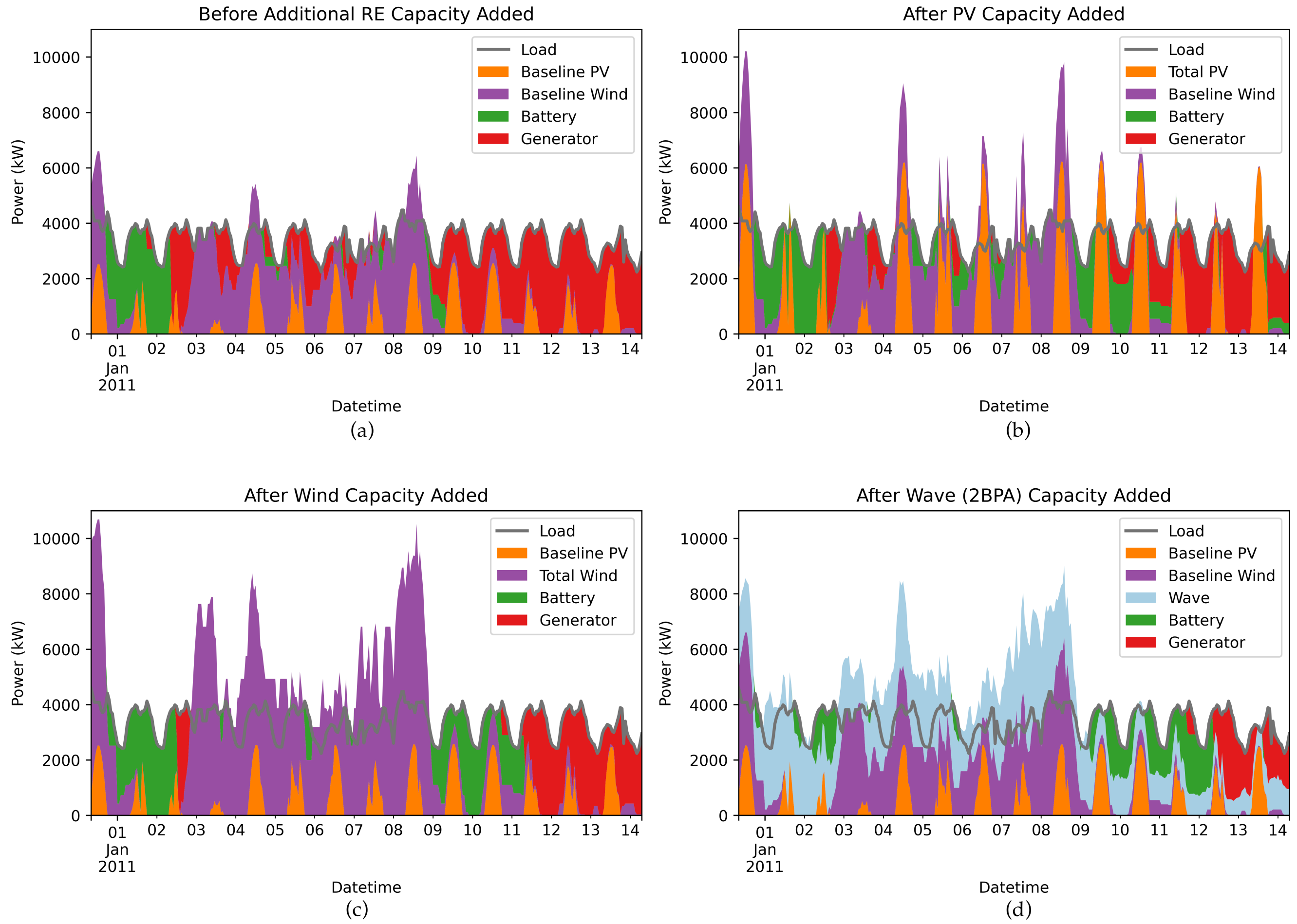

Fig. 4. Microgrid dispatch operation for (a) the baseline system, (b) the baseline system with 5 MW of PV capacity added, (c) the baseline system with 5 MW of wind capacity added, and (d) the baseline system with 5 MW of wave capacity added (2BPA). In all four plots, the load is shown by the gray line, PV generation in orange, wind production in purple, battery discharge energy in green, biofuel generator production in red, and wave generation in blue.

TABLE III
PERCENT REDUCTION IN REQUIRED BATTERY CAPACITY BY ADDING WIND OR WAVE CAPACITY INSTEAD OF PV CAPACITY

	Wind	Wave (BBDB)	Wave (2BPA)
100% zero-emission generation	11%	7%	17%

B. Battery capacity required for zero-emissions

For the second simulation set, a fixed amount of renewable energy capacity (5 MW) was added to the baseline microgrid system, and the battery capacity and power were increased until 100% zero-emission generation was achieved or a threshold battery capacity (211 MWh) was reached. Table III shows the percent reduction in the required overall battery capacity if wind or wave capacity is added to the baseline system instead of PV. Adding wind or wave capacity to the baseline microgrid instead of more PV capacity results in a smaller required increase in battery capacity to achieve 100% zero-emission generation.

C. Biofuel requirements for fixed additional renewable capacity

The last set of simulations compared the biofuel requirements of the microgrid after adding 5 MW of additional renewable energy capacity from the different resource types. The required biofuel generation capacity and fuel consumption for a 14-day outage period were calculated (see Table IV as well as the SRE ratio and the improvement of that ratio over the baseline system (see Table V). Adding either wind or wave resources results in a significantly smaller required biofuel generator capacity requirement and fuel use as compared with using more PV resources, with the 2BPA wave profile performing the best and maximizing fuel cost savings over the 2-week analysis period. Both wind and wave resources have a significant impact on the SRE ratio as compared with PV, likely due to the ability to better use the battery with more diverse resource generation.

IV. DISCUSSION

The results of this analysis demonstrate how marine energy resources could theoretically supplement and enhance the Moloka'i microgrid. In particular, this analysis demonstrated that incorporating either wind

TABLE IV
PERCENT REDUCTION IN REQUIRED GENERATOR CAPACITY, FUEL USE, AND FUEL COST BY ADDING WIND OR WAVE CAPACITY INSTEAD OF PV CAPACITY (2-WEEK PERIOD)

	Wind	Wave (BBDB)	Wave (2BPA)
Generator capacity	34%	32%	66%
Fuel use	46%	37%	62%
Fuel cost savings	$14,400	$12,200	$17,900
Fuel cost savings (yr.)	$374,400	$317,200	$465,400

or wave resources into a baseline PV, wind, battery energy storage, and biofuel microgrid requires a significantly lower additional capacity (15-47% less) to meet a zero-emission generation goal of 95% or 100% as compared with adding more PV, demonstrating the benefits of resource diversification. The benefits of adding wind or wave resources depend on the wave generation profile used and the specific metric in question.

For example, when adding renewable capacity to reach 95% or 100% zero-emission generation, one of the wave profiles required the smallest additional capacity, followed by the wind profile, and then the other wave profile. However, additional wave capacity from either profile resulted in the microgrid being able to meet the zero-emission generation goal for a greater number of outage scenarios as compared with the wind profile. This indicates that adding wave resources to the baseline microgrid instead of more PV or wind capacity provided more certainty that electrical load would be met across a large range of conditions, without the need for backup biofuel generation. Thus there is a trade-off between minimizing the risk of a load shortfall and decreasing the cost of the installed system.

The specific results reported here, in which the 2BPA wave energy production profile allowed the greatest increase in zero-emission generation for the smallest additional capacity as compared with a wind profile or a different wave profile, are strongly dependent on the modeling choices for both wave and wind profiles, as well as the location of the site and the chosen battery model parameters. In this analysis, the 2BPA technology out-performed the BBDB technology, likely as a direct result of the 20% larger annual generation for the 2BPA production profile as compared with the BBDB profile. However, different types of generation might be more suitable for meeting a zero-emission microgrid goal with different underlying assumptions. The key take-away here is that a diverse set of resources allows for more certainty that a microgrid can consistently power a system without the need for an emission-generating, dispatchable resource, such as biofueled generators, or without over-sizing the system. For island microgrids, marine renewable resources provide a convenient source of complementary power.

This paper introduces an approach for evaluating the fitness of different resources for meeting zero-emission goals in a microgrid and reducing over-sizing. This methodology could be applied to specific sites and regions to help evaluate the optimal mix of resources and demonstrate the benefits of introducing additional, complementary sources of generation.

V. CONCLUSIONS

Greater diversity of renewable resources that produce power in complementary periods creates a more redundant, resilient microgrid and, when properly proportioned, less overall required generation capacity. Diversity of resources therefore has implications for electric system costs, efficient operation, and maintenance of electric service during outages. In particular this analysis illustrates how marine energy resources, specifically wave resources, by virtue of generation profiles that are not coincident with PV and wind profiles can offer microgrids higher levels of reliability and resilience. These considerations are significant for remote grids and island grids, which cannot lean on a larger grid or readily available fuels when traditional service is disrupted. This analysis is also revealing for microgrids, which are designed to provide extra layers of security in electric service for critical loads over long periods of disruption.

ACKNOWLEDGEMENT

The authors wish to express their gratitude for the sponsorship and guidance of Simon Gore with the Water Power Technologies Office at the U.S. Department of Energy as well as Steve DeWitt formerly of the Water Power Technologies Office for his longtime support and guidance of this work. The authors would also like to thank Travis Douville and Cary Counts for a thoughtful and thorough review of this paper.

REFERENCES

[1] G. Reikard, B. Robertson, and J.-R. Bidlot, "Combining wave energy with wind and solar: Short-term forecasting," *Renewable Energy*, vol. 81, no. C, pp. 442–456, 2015. [Online]. Available: https://EconPapers.repec.org/RePEc:eee:renene:v:81:y:2015:i:c:p:442-456

[2] I. Moazzen, B. Robertson, P. Wild, A. Rowe, and B. Buckham, "Impacts of large-scale wave integration into a transmission-constrained grid," *Renewable Energy*, vol. 88, pp. 408–417, 2016. [Online]. Available: https://www.sciencedirect.com/science/article/pii/S0960148115304705

[3] B. Robertson, J. Bekker, and B. Buckham, "Renewable integration for remote communities: Comparative allowable cost analyses for hydro, solar and wave energy," *Applied Energy*, vol. 264, p. 114677, 2020. [Online]. Available: https://www.sciencedirect.com/science/article/pii/S0306261920301896

[4] "Water power technologies office projects map," 2020, online; accessed 22-February-2021]. [Online]. Available: https://www.energy.gov/eere/water/water-power-technologies-office-projects-map

[5] B. Robertson, "Ocean wave energy generation on the west coast of vancouver island and the queen charlotte islands," *Guelph Engineering Journal*, vol. 3, 01 2010.

[6] K. Simonsen and B. A. Niclasen, "Analysis of the energy potential of tidal streams on the faroe shelf," *Renewable Energy*, vol. 163, pp. 836–844, 2021. [Online]. Available: https://www.sciencedirect.com/science/article/pii/S0960148120313689

[7] H. M. Tróndheim, B. A. Niclasen, T. Nielsen, F. F. D. Silva, and C. L. Bak, "100% sustainable electricity in the faroe islands: Expansion planning through economic optimization," *IEEE Open Access Journal of Power and Energy*, vol. 8, pp. 23–34, 2021.

[8] "Faroe islands – tidal energy to reach 100% renewable by 2030." [Online]. Available: https://www.minesto.com/projects/faroe-islands

TABLE V
AVERAGE SRE AMONG SIMULATIONS (2-WEEK PERIOD)

	Base system	+PV	+Wind	+wave (BBDB)	+wave (2BPA)
SRE	0.51	0.79	0.93	0.90	0.96
ΔSRE from baseline	-	+0.27	+0.42	+0.39	+0.45

[9] M. Majidi Nezhad, D. Groppi, F. Rosa, G. Piras, F. Cumo, and D. A. Garcia, "Nearshore wave energy converters comparison and mediterranean small island grid integration," *Sustainable Energy Technologies and Assessments*, vol. 30, pp. 68–76, 2018. [Online]. Available: https://www.sciencedirect.com/science/article/pii/S221313881830016X

[10] D. Preziuso, G. García-Medina, R. O'Neil, Z. Yang, and T. Wang, "Evaluating the potential for tidal phase diversity to produce smoother power profiles," *Journal of Marine Science and Engineering*, vol. 8, no. 4, 2020. [Online]. Available: https://www.mdpi.com/2077-1312/8/4/246

[11] Hawaiian Electric Company, "Psip update report: December 2016," 2016. [Online]. Available: https://www.hawaiianelectric.com/documents/clean_energy_hawaii/grid_modernization/dkt_2014_0183_20161223_companies_PSIP_update_report_1_of_4.pdf

[12] J. E. Stopa, J.-F. Filipot, N. Li, K. F. Cheung, Y.-L. Chen, and L. Vega, "Wave energy resources along the hawaiian island chain," *Renewable Energy*, vol. 55, pp. 305–321, 2013. [Online]. Available: https://www.sciencedirect.com/science/article/pii/S0960148112007963

[13] Y. Yuan, P. J. Balducci, K. Mongird, V. Fotedar, D. Wu, and D. Bhatnagar, "Hawaiian Electric Companies Demand Response Tool," Tech. Rep., 2019. [Online]. Available: https://www.osti.gov/biblio/1648191

[14] R. Gelaro *et al.*, "The modern-era retrospective analysis for research and applications, version 2 (merra-2)," *Journal of Climate*, vol. 30, pp. 5419–5454, 2017.

[15] Hawaiian Electric Company, "Maui electric issuing largest call for renewable energy projects for moloka'i, lāna'i," 2019. [Online]. Available: https://www.hawaiianelectric.com/documents/about_us/news/2019_maui_electric/20191202_maui_electric_issues_request_for_proposals_molokai_lanai.pdf

[16] Northern Power Systems, "Npc 100c-24 class iii." [Online]. Available: http://windup.pt/resources/BrochureNPS100-24.pdf

[17] Z. Yang, G. García-Medina, W.-C. Wu, and T. Wang, "Characteristics and variability of the nearshore wave resource on the us west coast," *Energy*, p. 117818, 2020.

[18] W.-C. Wu, T. Wang, Z. Yang, and G. García-Medina, "Development and validation of a high-resolution regional wave hindcast model for u.s. west coast wave resource characterization," *Renewable Energy*, vol. 152, pp. 736–753, 2020. [Online]. Available: https://www.sciencedirect.com/science/article/pii/S0960148120300963

[19] B. Robertson, H. Bailey, M. Leary, and B. Buckham, "A methodology for architecture agnostic and time flexible representations of wave energy converter performance," *Applied Energy*, vol. 287, p. 116588, 2021. [Online]. Available: https://www.sciencedirect.com/science/article/pii/S030626192100132X

[20] H. Bailey, B. R. Robertson, and B. J. Buckham, "Wave-to-wire simulation of a floating oscillating water column wave energy converter," *Ocean Engineering*, vol. 125, pp. 248–260, 2016. [Online]. Available: https://www.sciencedirect.com/science/article/pii/S0029801816303444

[21] H. Bailey, B. Robertson, and B. Buckham, "Variability and stochastic simulation of power from wave energy converter arrays," *Renewable Energy*, vol. 115, pp. 721–733, 2018. [Online]. Available: https://www.sciencedirect.com/science/article/pii/S0960148117308108

[22] S. Newman, K. Shiozawa, J. Follum, E. Barrett, T. Douville, T. Hardy, and A. Solana, "A comparison of pv resource modeling for sizing microgrid components," *Renewable Energy*, vol. 162, pp. 831 – 843, 2020. [Online]. Available: http://www.sciencedirect.com/science/article/pii/S0960148120313197

[23] A. P. Reiman, J. S. Homer, B. Bhattarai, and A. C. Orrell, "Quantifying technical diversity benefits of wind as a distributed energy resource," in *2020 IEEE Power Energy Society Innovative Smart Grid Technologies Conference (ISGT)*, 2020, pp. 1–5.

[24] U.S. Environmental Protection Agency, "Emission factors for greenhouse gas inventories." [Online]. Available: https://www.epa.gov/sites/default/files/2018-03/documents/emission-factors_mar_2018_0.pdf

[25] U.S. Department of Energy Alternative Fuels Data Center, "Alternative fuels data center fuel properties comparison." [Online]. Available: https://afdc.energy.gov/files/u/publication/fuel_comparison_chart.pdf